



BNL-104927-2016-JA

**Spatially resolved ultrafast  
magnetic dynamics initiated at  
a complex oxide heterointerface**

*M. Foerst*

*Submitted to Nature Materials*

September 2015

**Condensed Matter Physics and Material Science Department**

**Brookhaven National Laboratory**

**U.S. Department of Energy  
[DOE Office of Science]**

Notice: This manuscript has been authored by employees of Brookhaven Science Associates, LLC under Contract No. DE-SC0012704 with the U.S. Department of Energy. The publisher by accepting the manuscript for publication acknowledges that the United States Government retains a non-exclusive, paid-up, irrevocable, world-wide license to publish or reproduce the published form of this manuscript, or allow others to do so, for United States Government purposes.

## **DISCLAIMER**

This report was prepared as an account of work sponsored by an agency of the United States Government. Neither the United States Government nor any agency thereof, nor any of their employees, nor any of their contractors, subcontractors, or their employees, makes any warranty, express or implied, or assumes any legal liability or responsibility for the accuracy, completeness, or any third party's use or the results of such use of any information, apparatus, product, or process disclosed, or represents that its use would not infringe privately owned rights. Reference herein to any specific commercial product, process, or service by trade name, trademark, manufacturer, or otherwise, does not necessarily constitute or imply its endorsement, recommendation, or favoring by the United States Government or any agency thereof or its contractors or subcontractors. The views and opinions of authors expressed herein do not necessarily state or reflect those of the United States Government or any agency thereof.

# **Spatially resolved ultrafast magnetic dynamics launched at a complex-oxide hetero-interface**

M. Först<sup>1\*</sup>, A.D. Caviglia<sup>2\*</sup>, R. Scherwitzl<sup>3</sup>, R. Mankowsky<sup>1</sup>, P. Zubko<sup>3</sup>, V. Khanna<sup>1,4,5</sup>,  
H. Bromberger<sup>1</sup>, S.B. Wilkins<sup>6</sup>, Y.-D. Chuang<sup>7</sup>, W.S. Lee<sup>8</sup>, W.F. Schlotter<sup>9</sup>, J.J. Turner<sup>9</sup>,  
G.L. Dakovski<sup>9</sup>, M.P. Minitti<sup>9</sup>, J. Robinson<sup>9</sup>, S.R. Clark<sup>10,4</sup>, D. Jaksch<sup>4,10</sup>, J.-M. Triscone<sup>3</sup>,  
J.P. Hill<sup>6</sup>, S.S. Dhesi<sup>5</sup>, and A. Cavalleri<sup>1,4</sup>

<sup>1</sup>*Max-Planck Institute for the Structure and Dynamics of Matter, Hamburg, Germany*

<sup>2</sup>*Kavli Institute of Nanoscience, Delft University of Technology, The Netherlands*

<sup>3</sup>*Département de Physique de la Matière Condensée, University of Geneva, Switzerland*

<sup>4</sup>*Department of Physics, Clarendon Laboratory, University of Oxford, UK*

<sup>5</sup>*Diamond Light Source, Chilton, Didcot, United Kingdom*

<sup>6</sup>*Condensed Matter Physics and Materials Science Department,  
Brookhaven National Laboratory, Upton, NY*

<sup>7</sup>*Advanced Light Source, Lawrence Berkeley Laboratory, Berkeley, CA*

<sup>8</sup>*The Stanford Institute for Materials and Energy Sciences (SIMES), Stanford Linear  
Accelerator Center (SLAC) National Accelerator Laboratory and Stanford University,  
Menlo Park, CA*

<sup>9</sup>*Linac Coherent Light Source, Stanford Linear Accelerator Center (SLAC) National  
Accelerator Laboratory, Menlo Park, CA*

<sup>10</sup>*Centre for Quantum Technologies, National University of Singapore, Singapore*

\*These authors contributed equally to this work.

Static strain in complex oxide heterostructures [1,2] has been extensively used to engineer electronic and magnetic properties at equilibrium [3]. In the same spirit, deformations of the crystal lattice with light may be used to achieve functional control across hetero-interfaces dynamically [4]. Here, by exciting large amplitude infrared-active vibrations in a  $\text{LaAlO}_3$  substrate we induce magnetic order melting in a  $\text{NdNiO}_3$  film across a hetero-interface. Femtosecond Resonant Soft X-ray Diffraction is used to measure the dynamics of the magnetic disordering, with sensitivity to the evolution both in space and time. We observe a magnetic melt front that grows from the substrate interface into the film, at a speed that suggests an electronically driven propagation mechanism. Light control at hetero-interfaces may lead to new opportunities in optomagnetism, for example by driving ultrafast domain wall motion to transport information across suitably designed devices.

In transition metal oxides, rearrangements in electronic and magnetic properties can be triggered by the application of magnetic [5] and electric fields [6], or pressure [7,8]. Switching has also been demonstrated in these materials using femtosecond optical excitation, at near-visible [9,10,11,12,13,14,15], mid-infrared [16,17,18,19,20], or THz [21,22,23] wavelengths.

Recently, selective excitation of lattice modes in the mid-infrared has been applied to complex oxide heterostructures, where the functional material can be separated from the optically excited region. By directly driving the infrared-active modes leading to structural distortions in the  $\text{LaAlO}_3$  substrate of a  $\text{LaAlO}_3/\text{NdNiO}_3$  heterostructure, an insulator-metal transition was triggered across the interface in the nickelate film [4].

Here, we apply time-resolved Resonant Soft X-ray Diffraction (RSXD) to measure the concomitant magnetic response in the  $\text{NdNiO}_3$  film with nanometer spatial and femtosecond temporal resolution. We find evidence of inhomogeneous magnetic melting dynamics, with a melt front that propagates from the interface into the  $\text{NdNiO}_3$  film. Theoretical considerations aid our interpretation that an insulator-metal transition launched locally at the hetero-interface could be driving this process by itinerant charges, which scramble magnetic order as they diffuse into the film.

Below about 200 K, metallic paramagnetic  $\text{NdNiO}_3$  undergoes a transition into a low-temperature antiferromagnetic insulating state [24,25]. This electronic and magnetic phase transition is concomitant with a structural transformation from an orthorhombic ( $\text{Pbnm}$ ) to a monoclinic ( $\text{P21/n}$ ) crystal structure. Further, the transition temperature depends on epitaxial strain [26], demonstrating sensitivity to lattice distortions.

We study a compressively strained film of 100 NdNiO<sub>3</sub> unit cells deposited on a (111) LaAlO<sub>3</sub> substrate by off-axis RF magnetron sputtering [27]. The low-temperature antiferromagnetic ordering on the Ni and Nd sublattices, shown schematically in Fig. 1(a), can be observed by RSXD at the pseudo-cubic (1/4 1/4 1/4) wave vector [28,29]. Figure 1(b) shows the static photon-energy dependent magnetic diffraction at this peak, measured at the Ni L<sub>2,3</sub> edges (data taken at I06 beamline of the Diamond Light Source synchrotron; see Ref. 30 for details).

Femtosecond RSXD experiments were carried out at the SXR beamline of the Linac Coherent Light Source free electron laser (FEL) [31]. Excitation pulses of 200 fs duration were tuned to 15 μm wavelength (82 meV photon energy), in resonance with the highest-frequency LaAlO<sub>3</sub> substrate phonon, which is well separated in energy from equivalent phonons of the NdNiO<sub>3</sub> film (see Figure 1(c)). We focused these mid-infrared pump pulses onto the sample with a fluence of 4 mJ/cm<sup>2</sup>. The sample was mounted on an in-vacuum diffractometer [32] and cooled to 40 K, i.e. into the antiferromagnetic insulating state. The FEL, which operated at 120 Hz repetition rate, was tuned to the 852 eV Ni L<sub>3</sub> edge. The bandwidth of the X-ray pulses was reduced to below 1 eV by a grating monochromator. Diffracted X-rays were detected as function of the time delay relative to the mid-infrared excitation pulses. An avalanche photodiode enabled pulse-to-pulse normalization of the diffracted to the incident light intensity.

Figure 1(d) shows the vibrationally induced intensity changes of the (1/4 1/4 1/4) diffraction peak, probing the antiferromagnetic order dynamics in the NdNiO<sub>3</sub> film. The peak intensity dropped by about 80 % within 1.6 ps and recovered on the few tens of picosecond time scale. In contrast to the case of direct interband excitation, for which the

antiferromagnetic peak dropped promptly [30], the 1.6 ps time constant for the initial reduction was significantly longer than the 250 fs time resolution of the experiment, where the latter is limited by the jitter between the FEL and the optical laser. We compare these dynamics to the time needed for the film to become metallic, as measured by the transient reflectivity in the 1–5 THz range induced by the same mid-infrared excitation (green dots in Fig. 1(d)). The two timescales, which reflect only average changes over the whole film, are comparable with one another, suggesting an intimate connection between the insulator-to-metal transition and the melting of magnetic order.

In Figure 2, we plot the transient  $\theta$ - $2\theta$  scans for the (1/4 1/4 1/4) diffraction peak, sensitive to the out-of-plane antiferromagnetic ordering. In equilibrium, i.e. at negative time delay, a narrow diffraction peak and Laue oscillations are observed, attesting to the presence of magnetic order across the entire 30-nm film height, with sharp magnetic boundaries.

Figure 2 further shows that a significant peak broadening and a disappearance of the Laue oscillations accompany the strong photo-induced reduction in peak intensity. The broadening of the diffraction peak indicates that the phonon excitation melts the magnetic order only over a fraction of the film along the sample growth direction. Further, the disappearance of the Laue oscillations indicates that the boundary between the ordered and disordered regions of the film is not sharp.

We also find that throughout these dynamics the in-plane correlation length, as measured by transverse rocking curves ( $\theta$  scans), remains unchanged (see Supplementary Information). Hence, the dynamics discussed here is one dimensional, evolving along the sample growth direction.

The spatial distribution of the magnetic order at a time delay  $\tau$  was analyzed quantitatively with the following expression for kinematic diffraction

$$I_{\tau}(q) \propto \left| \int_0^D F(z, \tau) e^{-iqz} dz \right|^2. \quad (1)$$

Here, the magnetic profile is represented by the space- and time-dependent structure factor  $F(z, \tau)$  along the sample growth direction  $z$ , with the magnitude of the scattering vector  $q = 4\pi \sin \theta / \lambda$  ( $\theta$  is the diffraction angle and  $\lambda$  the x-ray wavelength) and  $D$  the film thickness.

Previous work has shown that these complex dynamics are initiated at the buried interface [4]. Also, the transient  $\theta$ - $2\theta$  scans show that the fraction of material, which is melted, increases with time and that the order-disorder interface becomes progressively smeared in time. Hence we chose a functional form  $F(z, \tau)$  that describes a soliton-like demagnetization front, propagating from the hetero-interface into the thin film:

$$F(z, \tau) = F_0 \cdot \left( \frac{1}{2} + \frac{1}{2} \operatorname{erf} \left( \frac{z - z_f(\tau)}{d_f(\tau)} \right) \right). \quad (2)$$

In this case,  $F_0$  is the equilibrium structure factor, and  $z_f$  and  $d_f$  are the time-dependent position and width of that phase front separating the unperturbed antiferromagnetic order from the disordered region of the film. Numerical fits of Eqs. (1) and (2) to the diffraction peak at selected time delays are shown as red solid lines in the lower panel of Fig. 2 and give excellent agreement with the data.

Figure 3(b) shows the corresponding early time scale evolution of the space-dependent magnetic order parameter, represented as  $|F(z, \tau)|^2$ . At negative time delays, the NdNiO<sub>3</sub> film is homogeneously ordered, with a sharp boundary at the hetero-interface. The mid-infrared excitation induces heterogeneous melting, with a demagnetizing phase front that

propagates halfway into the film – before coming to a stop at ~2 ps. This phase front leaves a magnetically disordered region behind, with a boundary between the two regions of about 10 nm width. The time-dependent position of the phase front is plotted in Figure 3(c), which indicates that the magnetic melt front propagates at a speed faster than the nominal longitudinal sound velocity ( $4.1 \times 10^3$  m/s) measured in an NdNiO<sub>3</sub> film by all-optical picosecond ultrasonics [33].

The long-term re-magnetization dynamics are shown in Figure 4. About 10 ps after the excitation, the demagnetized part of the film starts recovering to the equilibrium state. Here, the phase front separating the photo-disordered from the unperturbed region of the film begins shifting back towards the substrate interface, and at the same time the domain boundary further broadens.

The heterogeneous dynamics discussed above are unique to the mid-infrared excitation of the substrate lattice. Near-infrared illumination of the same heterostructure at 800 nm, which involves significant homogeneous charge excitation in the nickelate film [30], shows that in this case the magnetic order is uniformly melted over the entire film. This can be clearly deduced from Figs. 5(a) and (b) unveiling that the 800-nm excitation reduces the intensity of the magnetic (1/4 1/4 1/4) diffraction without noticeable change in the peak width. The same fitting procedure as applied above for the mid-infrared substrate excitation (see also the red solid lines in Figure 5(b)), shows the uniform and instantaneous decrease of the magnetic order parameter across the whole film thickness.

We next turn to a discussion of the physics underlying the non-uniform magnetic order melting observed under mid-infrared excitation.

We can exclude direct absorption of the mid-IR pump pulse in the nickelate film as being responsible for the observed magnetization dynamics. This is not only because the energy deposited in the nickelate is negligible (3% of the incident energy). Indeed, the penetration depth in NdNiO<sub>3</sub> is approximately 1- $\mu$ m at the pump wavelength (see Fig. 1(c)), which also implies that the 30-nm thick film would have to be driven homogeneously.

The speed of the phase front extracted from our fits is time dependent, and is as high as 1.7 times the longitudinal sound velocity measured in Ref. 33. One can then conclude that heat from the substrate, never exceeding a few degree heating [4], cannot be causing the effect observed here by propagation into the film. One could envisage a structural phase transition occurring at the buried interface and propagating inward, thereby making the nickelate metallic and melting the magnetism along the way. This would be an intriguing explanation for the data, although a structural phase transition always propagates at a velocity smaller than the speed of sound [34]. Finally, despite our conclusion that the front propagates at speeds higher than the speed of sound, inaccuracies in the exact functional form of the fit function fit or differences in the speed of sound between the bulk and the film may make this assignment tentative. Hence, we also discuss if a propagating acoustic pulse may be the driving mechanism for the heterogeneous phase dynamics. However, it is not clear how resonant excitation of a  $q \sim 0$  optical phonon mode could launch a propagating strain pulse at this speed. Furthermore, the small strain observed ( $< 10^{-3}$ ) appears unlikely to rearrange the magnetism alone. One would rather expect a cascade of slower scattering processes for this to happen.

Rather, we propose that the direct excitation of the substrate lattice induces octahedral distortions [35,36] across the interface that then act on the electronic and magnetic ordering of the nickelate film. Such a scenario of inhomogeneous lattice distortion profiles has been predicted for perovskite heterostructures in the static case [37]. Near the interface, this effect could locally quench the exchange interaction or drive an insulator-metal transition to launch the heterogeneous phase change.

Propagation of the phase is not easily attributed to magnetic excitations advancing into the film. The anisotropic magnetic interaction stabilizing the Neel order will introduce a gap and flatten the dispersion of magnons (see Supplemental Material for details), resulting in reduced group velocity and magnon localization.

The concomitant insulator-metal transition appears to be a more probable cause for the phase front propagation. Charge carriers, made mobile at the interface are very efficient at randomizing spin correlations [38] and have kinetic energies, which exceed magnetic energy scales and which can sustain a front that propagates. The scrambling of antiferromagnetic order would transfer initial kinetic energy into the magnetic sector [39] eventually leading to a stalling of the phase front. Although a mechanistic description of this process requires materials specific calculations [40,41], which are beyond the scope of the present paper, a model Hamiltonian description, in which charges are freed at the interface and are mobile through diffusion (see Supplemental Material), confirms these qualitative arguments. This scenario is also compatible with the similar time scales observed for the insulator-metal transition and the magnetic order melting presented in Fig. 1(d).

In summary, we have shown that the dynamics of magnetic disordering in complex oxide heterostructures follows distinctly new physical pathways when the substrate lattice is excited, in contrast to the case in which direct charge excitations in the functional film are involved. We demonstrate that the melting is initiated at the interface and propagates into the film, and assign the underlying physics to electronic processes. We note that the ability to control magnetic phase fronts, or even domain walls, with light in different constituents of a heterostructure may be conducive to new applications in optomagnetic devices, which may encode information in domain walls that are shuttled by optical stimulation and may even support higher bit rates than spin torque driven walls [42].

## **ACKNOWLEDGEMENT**

We thank A. Frano for helpful discussions.

Portions of this research were carried out on the SXR Instrument at the Linac Coherent Light Source (LCLS), a division of SLAC National Accelerator Laboratory and an Office of Science user facility operated by Stanford University for the U.S. Department of Energy. The SXR Instrument is funded by a consortium whose membership includes the LCLS, Stanford University through the Stanford Institute for Materials Energy Sciences (SIMES), Lawrence Berkeley National Laboratory (LBNL, contract No. DE-AC02-05CH11231), University of Hamburg through the BMBF priority program FSP 301, and the Center for Free Electron Laser Science (CFEL).

The research leading to these results has received funding from the European Research Council under the European Union's Seventh Framework Programme (FP7/2007-2013) / ERC Grant Agreement n° 319286 (Q-MAC) and n°281403 (FEMTOSPIN). Work at Brookhaven National Laboratory was funded by the Department of Energy, Division of Materials Science and Engineering under contract No. DE-AC02-98CH10886.

## **AUTHOR CONTRIBUTIONS**

A.D.C., M.F. and A.C. conceived this project. M.F., A.D.C., R.M., V.K., S.B.W., S.S.D., and J.P.H performed the experiment at the LCLS, supported by W.F.S., J.J.T. and G.L.D (beamline), M.P.M. and J.R. (laser), Y.D.C and W.S.L. (experimental endstation). The sample was grown by R.S., P.Z., and J.M.T.. M.F. analyzed the data with help from H.B.. S.R.C and D.J. provided the model Hamiltonian theory. M.F., A.D.C. and A.C. wrote the manuscript, with feedback from all co-authors.

## FIGURE CAPTIONS

### **Fig. 1. Magnetic ordering in NdNiO<sub>3</sub> and the vibrationally induced phase transition**

(a) Visualization of the complex antiferromagnetic ordering in NdNiO<sub>3</sub>. (b) Energy scan of the (1/4 1/4 1/4) diffraction peak, associated with the magnetic order on the Ni sublattice, around the Ni L<sub>2,3</sub> edges. These data are measured on the NdNiO<sub>3</sub>/LaAlO<sub>3</sub> heterostructure. (c) Wavelength dependent penetration depth of mid-infrared light around the NdNiO<sub>3</sub> (green) and LaAlO<sub>3</sub> (blue) high-frequency phonon resonances. The energy spectrum of the excitation pulses at 15 μm wavelength (black data points, fitted by a Gaussian profile in red) is tuned in resonance with the substrate mode. (d) Blue: Changes of the peak intensity of the Ni L<sub>3</sub> diffraction peak at 852 eV, following this optical excitation with a fluence of 4 mJ/cm<sup>2</sup>. The green data points show the transient THz reflectivity of the same sample under identical excitation conditions. The melting of the magnetic order and the insulator-metal transition both take place on the same time scale.

### **Fig. 2: Temporal evolution of the antiferromagnetic order in reciprocal space**

(a) Photo-induced dynamics of the momentum dependence of the (1/4 1/4 1/4) Ni L<sub>3</sub>-edge diffraction peak (logarithmic scale), on both short and long time scales. (b) The same diffraction peak at selected time delays before and after the mid-infrared excitation, overlaid with numerical fits assuming a heterogeneous melting of the antiferromagnetic order triggered at the NdNiO<sub>3</sub>/LaAlO<sub>3</sub> interface.

### **Fig. 3: Real space dynamics of the antiferromagnetic order**

(a) Schematic illustration of the demagnetization process. At negative time delay, the NdNiO<sub>3</sub> film is homogeneously ordered. Direct excitation of a substrate phonon triggers a magnetic “melt” front, propagating from the interface into the film. (b) Short time scale spatial

dynamics of the magnetic order parameter along the [111] direction, extracted from the numerical fits shown in Figure 2. (c) Centre position of the phase front, separating the melted from the unperturbed region of the film (blue dots). The striped area marks the sonic regime, given by the  $4.1 \times 10^3$  m/s NdNiO<sub>3</sub> longitudinal speed of sound according to Ref. 33.

**Fig. 4: Recovery dynamics of the antiferromagnetic order** (a) Three-dimensional plot of the long time scale spatial dynamics of the magnetic order parameter. The recovery to the equilibrium state takes place on the time scale of 100 ps. (b) Time-dependent position and width of the magnetic phase front, extracted from the data shown in panel (a).

**Fig. 5: Magnetization dynamics following Ni charge transfer excitation at 800 nm** (a) Photo-induced dynamics of the (1/4 1/4 1/4) Ni L<sub>3</sub>-edge diffraction peak in reciprocal space (logarithmic intensity scale). The excitation fluence is about 4 mJ/cm<sup>2</sup>. (b) The same diffraction peak at selected time delays before and after the near-infrared excitation, together with numerical fits (red solid lines) of Eqs. (1) and (2). (b) Three-dimensional plot of the spatiotemporal dynamics of the magnetic order parameter, showing homogeneous photo-induced demagnetization.

# FIGURES

Figure 1

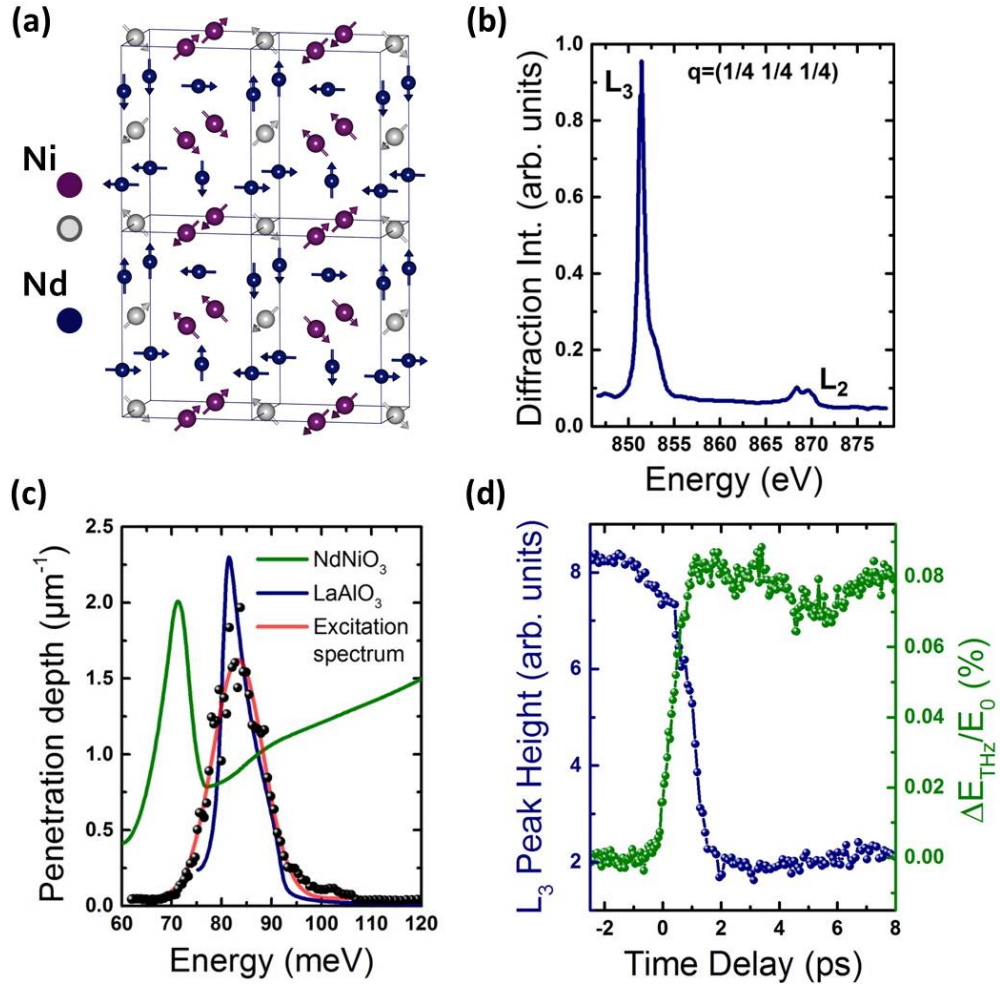


Figure 2

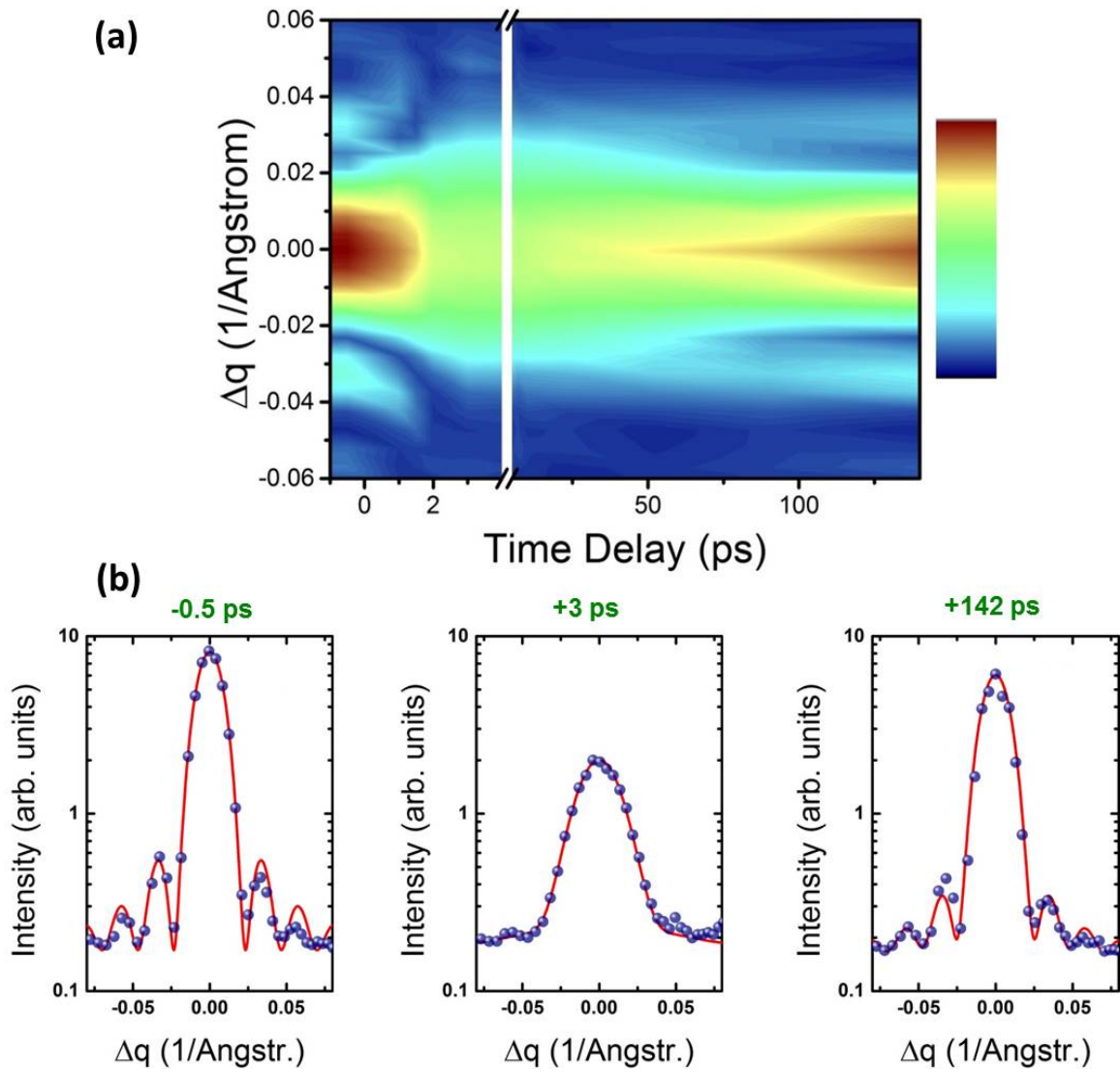


Figure 3

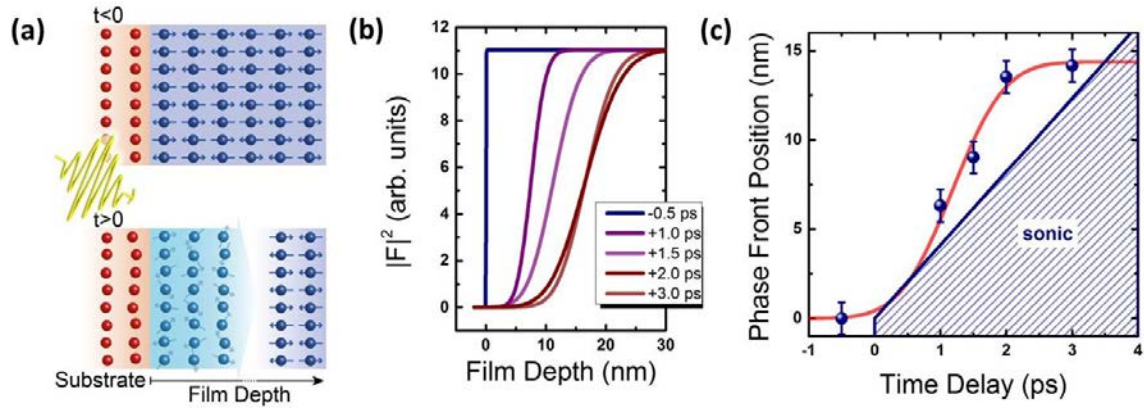


Figure 4

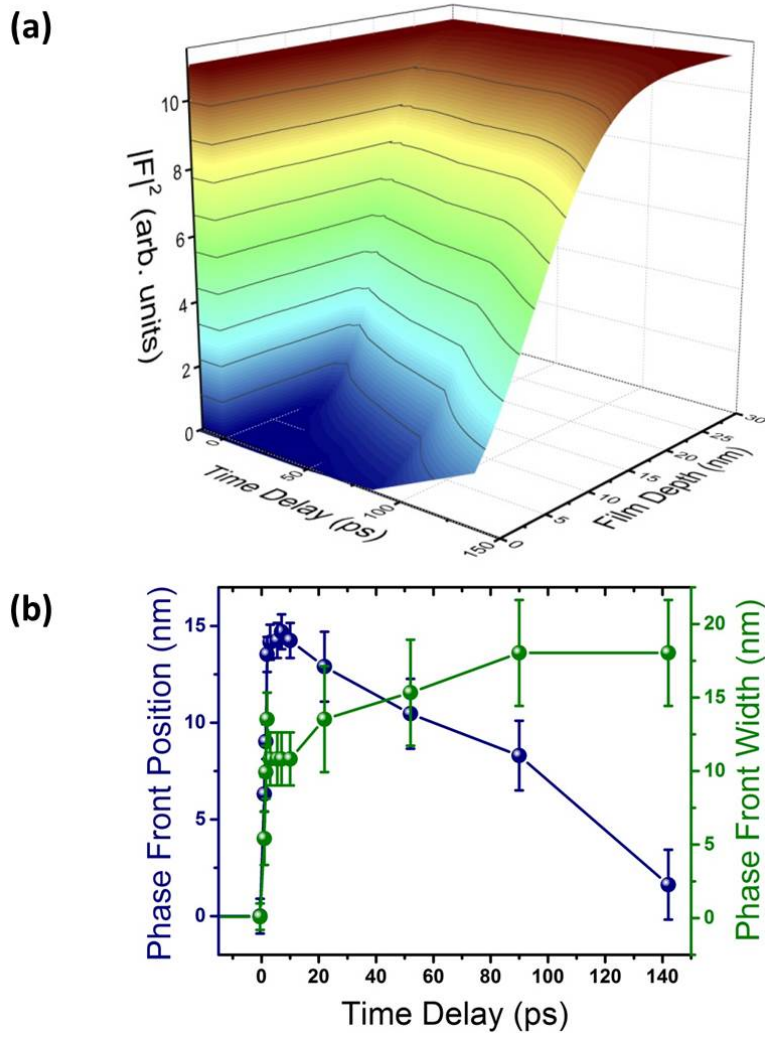
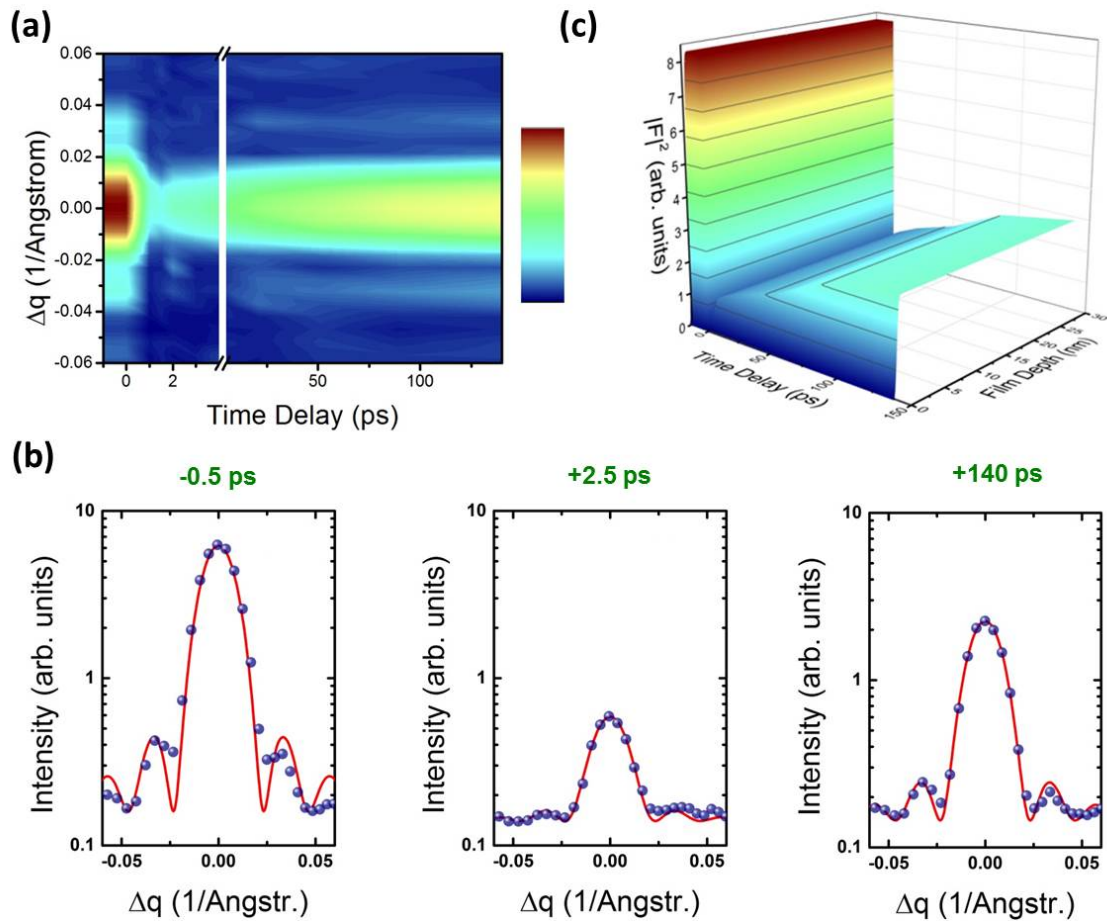


Figure 5

Near-infrared excitation at 800nm



## REFERENCES

- 
- [1] J.H. Haeni, P. Irvin, W. Chang, R. Uecker, P. Reiche, Y.L. Li, S. Choudhury, W. Tian, M.E. Hawley, B. Craigo, A.K. Tagantsev, X.Q. Pan, S.K. Streier, L.Q. Chen, S.W. Kirchoefer, J. Levy, and D.G. Schlom, “Room-temperature ferroelectricity in strained SrTiO<sub>3</sub>“, Nature **430**, 758 (2004).
- [2] J.H. Lee, L. Fang, E. Vlahos, X. Ke, Y.W. Jung, L.F. Kourkoutis, J.-W. Kim, P.J. Ryan, T. Heeg, M. Roeckerath, V. Goian, M. Bernhagen, R. Uecker, P.C. Hammel, K. M. Rabe, S. Kamba, J. Schubert, J.W. Freeland, D.A. Muller, C. J. Fennie, P. Schier, V. Gopalan, E. Johnston-Halperin, and D.G. Schlom, “A strong ferroelectric ferromagnet created by means of spin–lattice coupling”, Nature **466**, 954 (2010).
- [3] H.Y. Hwang, Y. Iwasa, M. Kawasaki, B. Keimer, N. Nagaosa, and Y. Tokura, “Emergent phenomena at oxide interfaces“, Nature Materials **11**, 103 (2012).
- [4] A.D. Caviglia, R. Scherwitzl, P. Popovich, W. Hu, H. Bromberger, R. Singla, M. Mitrano, M.C. Hoffmann, S. Kaiser, P. Zubko, S. Gariglio, J.-M. Triscone, M. Först, and A. Cavalleri, “Ultrafast strain engineering in complex oxide heterostructures“, Phys. Rev. Lett **108**, 136801 (2012).
- [5] Y. Tomioka, A. Asamitsu, H. Kuwahara, Y. Moritomo, and Y. Tokura, “Magnetic-field-induced metal-insulator phenomena in Pr<sub>1-x</sub>Ca<sub>x</sub>MnO<sub>3</sub> with controlled charge-ordering instability”, Phys. Rev. B **53**, R1689 (1996).
- [6] A. Asamitsu, Y. Tomioka, H. Kuwahara and Y. Tokura, Nature **388**, 50 (1997).
- [7] H.Y. Hwang, S.-W. Cheong, P.G. Radaelli, M. Marezio, and B. Batlogg, “Lattice effects on the magnetoresistance in doped LaMnO<sub>3</sub>”, Phys. Rev. Lett. **75**, 914 (1995).

- 
- [8] P.C. Canfield, J.D. Thompson, S.-W. Cheong, and L.W. Rupp, “Extraordinary pressure dependence of the metal-to-insulator transition in the charge-transfer compounds  $\text{NdNiO}_3$  and  $\text{PrNiO}_3$ ”, *Phys. Rev. B* **47**, 12357 (1993).
- [9] K. Miyano, T. Tanaka, Y. Tomioka, and Y. Tokura, “Photoinduced insulator-to-metal transition in a perovskite manganite”, *Phys. Rev. Lett.* **78**, 4257 (1997).
- [10] A. Cavalleri, Cs. Toth, C.W. Siders, J.A. Squier, F. Raksi, P. Forget, and J.C. Kieffer, “Femtosecond structural dynamics in  $\text{VO}_2$  during an ultrafast solid-solid phase transition”, *Phys. Rev. Lett.* **87**, 237401 (2001).
- [11] L. Perfetti, P.A. Loukakos, M. Lisowski, U. Bovensiepen, H. Berger, S. Biermann, P.S. Cornaglia, A. Georges, and M. Wolf, “Time evolution of the electronic structure of  $1\text{T-TaS}_2$  through the insulator-metal transition”, *Phys. Rev. Lett.* **97**, 067402 (2006).
- [12] K.W. Kim, A. Pashkin, H. Schäfer, M. Beyer, M. Porer, T. Wolf, C. Bernhard, J. Demsar, R. Huber, and A. Leitenstorfer, “Ultrafast transient generation of spin-density-wave order in the normal state of  $\text{BaFe}_2\text{As}_2$  driven by coherent lattice vibrations”, *Nature Materials* **11**, 497 (2012)
- [13] S.L. Johnson, R.A. de Souza, U. Staub, P. Beaud, E. Moehr-Vorobeva, G. Ingold, A. Caviezel, V. Scagnoli, W. F. Schlotter, J. J. Turner, O. Krupin, W. S. Lee, Y. D. Chuang, L. Patthey, R. G. Moore, D. Lu, M. Yi, P. S. Kirchmann, M. Trigo, P. Denes, D. Doering, Z. Hussain, Z. X. Shen, D. Prabhakaran, and A. T. Boothroyd, “Femtosecond dynamics of the collinear-to-spiral antiferromagnetic phase transition in  $\text{CuO}$ ”, *Phys. Rev. Lett.* **108**, 037203 (2012).
- [14] W. S. Lee, Y. D. Chuang, R. G. Moore, Y. Zhu, L. Patthey, M. Trigo, D. H. Lu, P. S. Kirchmann, O. Krupin, M. Yi, M. Langner, N. Huse, J. S. Robinson, Y. Chen, S. Y.

---

Zhou, G. Coslovich, B. Huber, D. A. Reis, R. A. Kaindl, R. W. Schoenlein, D. Doering, P. Denes, W. F. Schlotter, J. J. Turner, S. L. Johnson, M. Först, T. Sasagawa, Y. F. Kung, A. P. Sorini, A. F. Kemper, B. Moritz, T. P. Devereaux, D.-H. Lee, Z. X. Shen, and Z. Hussain, “Phase fluctuations and the absence of topological defects in a photo-excited charge-ordered nickelate“, *Nature Communications* **3**, 838 (2012).

[15] S. de Jong et al., “Speed limit of the insulator-metal transition in magnetite”, *Nature Materials* **12**, 882 (2013).

[16] M. Rini, R. Tobey, N. Dean, J. Itatani, Y. Tomioka, Y. Tokura, R.W. Schoenlein, and A. Cavalleri, “Control of the electronic phase of a manganite by mode-selective vibrational excitation”, *Nature* **449**, 72 (2007).

[17] R.I. Tobey, R. Prabakaran, A.T.J. Boothroyd, and A. Cavalleri, “Ultrafast electronic phase transition in  $\text{La}_{1/2}\text{Sr}_{3/2}\text{MnO}_4$  by coherent vibrational excitation: Evidence for nonthermal melting of orbital order”, *Phys. Rev. Lett.* **101**, 197404 (2008).

[18] M. Först, R. Tobey, S. Wall, H. Bromberger, V. Khanna, A. Cavalieri, Y.-D. Chuang, W. Lee, R. Moore, W. Schlotter, J. Turner, O. Krupin, M. Trigo, H. Zheng, J. Mitchell, S. Dhesi, J. Hill, and A. Cavalleri, “Driving magnetic order in a manganite by ultrafast lattice excitation”, *Phys. Rev. B* **84**, 241104R (2011).

[19] D. Fausti R.I. Tobey, N. Dean, S. Kaiser, A. Dienst, M.C. Hoffmann, S. Pyon, T. Takayama, H. Takagi, and A. Cavalleri, “Light-induced superconductivity in a stripe-ordered cuprate”, *Science* **331**, 189 (2011).

[ 20 ] S. Kaiser, D. Nicoletti, C.R. Hunt, W. Hu, I. Gierz, H.Y. Liu, M. Le Tacon, T. Loew, D. Haug, B. Keimer, and A. Cavalleri, “Light-induced inhomogeneous superconductivity far above  $T_c$  in  $\text{YBa}_2\text{Cu}_3\text{O}_{6+x}$ ”, arXiv 1205.4661 (2012); W. Hu,

---

I. Gierz, D. Nicoletti, S. Kaiser, C. R. Hunt, M. C. Hoffmann, M. Först, V. Khanna, T. Loew, M. Le Tacon, B. Keimer, A. Cavalleri, “Enhancement of superconductivity by redistribution of interlayer coupling in optically stimulated  $\text{YBa}_2\text{Cu}_3\text{O}_{6.5}$ ”, arXiv 1308.3204 (2013).

[21] A. Dienst, M.C. Hoffmann, D. Fausti, J.C. Petersen, S. Pyon, T. Takayama, H. Takagi, and A. Cavalleri, “Bi-directional ultrafast electric-field gating of interlayer charge transport in a cuprate superconductor”, *Nature Photonics* **5**, 485 (2011).

[22] T. Kampfrath, A. Sell, G. Klatt, A. Pashkin, S. Mährlein, T. Dekorsy, M. Wolf, M. Fiebig, A. Leitenstorfer, and R. Huber, “Coherent terahertz control of antiferromagnetic spin waves“, *Nature Photonics* **5**, 31 (2011).

[23] M.K. Liu, H.Y. Hwang, H. Tao, A.C. Strikwerda, K.B. Fan, G.R. Keiser, A.J. Sternbach, K.G. West, S. Kittiwatanakul, J.W. Lu, S.A. Wolf, F.G. Omenetto, X. Zhang, K.A. Nelson, and R.D. Averitt, “Terahertz-field-induced insulator-to-metal transition in vanadium dioxide metamaterial“, *Nature* **487**, 345 (2012).

[24] M.L. Medarde, “Structural, magnetic and electronic properties of  $\text{RNiO}_3$  perovskites (R = rare earth)”, *Journal of Physics Condensed Matter* **9**, 1679 (1997).

[25] G. Catalan, “Progress in perovskite nickelate research”, *Phase Transitions* **81**, 729 (2008).

[26] G. Catalan, R. M. Bowman, and J. M. Gregg, “Metal-insulator transitions in  $\text{NdNiO}_3$  thin films”, *Phys. Rev. B* **62**, 7892 (2000).

[27] R. Scherwitzl, P. Zubko, I.G. Lezama, S. Ono, A.F.Morpurgo, G. Catalan, and J.-M. Triscone, “Electric-field control of the metal-insulator transition in ultrathin  $\text{NdNiO}_3$  films”, *Advanced Materials* **22**, 5517 (2010).

- 
- [28] V. Scagnoli, U. Staub, M. Janousch, A. Mulders, M. Shi, G. Meijer, S. Rosenkranz, S. Wilkins, L. Paolasini, J. Karpinski, S. Kazakov, and S. Lovesey, “Charge disproportionation and search for orbital ordering in NdNiO<sub>3</sub> by use of resonant x-ray diffraction”, *Phys. Rev. B* **72**, 155111 (2005).
- [29] V. Scagnoli, U. Staub, Y. Bodenthin, M. Garcia Fernandez, A. Mulders, G. Meijer, and G. Hammerl, “Induced noncollinear magnetic order of Nd<sup>3+</sup> in NdNiO<sub>3</sub> observed by resonant soft x-ray diffraction”, *Phys. Rev. B* **77** 115138 (2008).
- [30] A.D. Caviglia, M. Först, R. Scherwitzl, V. Khanna, H. Bromberger, R. Mankowsky, R. Singla, Y.-D. Chuang, W.S. Lee, O. Krupin, W.F. Schlotter, J.J. Turner, G.L. Dakovski, M.P. Minitti, J. Robinson, V. Scagnoli, S.B. Wilkins, S.A. Cavill, M. Gibert, S. Gariglio, P. Zubko, J.-M. Triscone, J.P. Hill, S.S. Dhesi, and A. Cavalleri, “Photoinduced melting of magnetic order in the correlated electron insulator NdNiO<sub>3</sub>” *Phys. Rev. B* **88**, 220401 (2013).
- [31] W.F. Schlotter, et al., „The soft x-ray instrument for materials studies at the linac coherent light source x-ray free-electron laser“, *Rev. Sci. Instrum.* **83**, 043107 (2012).
- [32] D. Doering, Y.-D. Chuang, N. Andresen, K. Chow, D. Contarato, C. Cummings, E. Domning, J. Joseph, J.S. Pepper, B. Smith, G. Zizka, C. Ford, W.S. Lee, M. Weaver, L. Patthey, J. Weizeorick, Z. Hussain, and P. Denes, *Rev. Sci. Instrum.* **82**, 073303 (2011).
- [33] P. Ruello, S. Zhang, P. Laffez, B. Perrin, and V. Gusev, “Laser-induced coherent acoustical phonons mechanisms in the metal-insulator transition compound NdNiO<sub>3</sub>: Thermal and nonthermal processes”, *Phys. Rev. B* **79**, 094303 (2009).

- 
- [34] K. Sokolowski-Tinten, J. Bialkowski, M. Boing, A. Cavalleri, and D. von der Linde, “Thermal and non-thermal melting of gallium arsenide after femtosecond laser excitation”, *Phys. Rev. B* **58**, 11805 (1998).
- [35] M. Först, C. Manzoni, S. Kaiser, Y. Tomioka, Y. Tokura, R. Merlin, and A. Cavalleri, “Nonlinear phononics as an ultrafast route to lattice control”, *Nature Physics* **7**, 854 (2011).
- [36] M. Först, R. Mankowsky, H. Bromberger, D.M. Fritz, H. Lemke, D. Zhu, M. Chollet, Y. Tomioka, Y. Tokura, R. Merlin, J.P. Hill, S.L. Johnson, and A. Cavalleri, “Displacive lattice excitation through nonlinear phononics viewed by femtosecond X-ray diffraction”, *Sol. State. Comm.* **169**, 24 (2013).
- [37] J. He, A. Borisevich, S.V. Kalinin, S.J. Pennycook, and S.T. Pantelidis, “Control of octahedral tilts and magnetic properties of perovskite oxide heterostructures by substrate symmetry”, *Phys. Rev. Lett.* **105**, 227203 (2010).
- [38] W.F. Brinkman and T.M. Rice, “Single-particle excitations in magnetic insulators”, *Phys. Rev. B* **2**, 1324 (1970).
- [39] L.N. Buleavskii, E.L. Nagaev and D.I. Khomskii, “A new type of auto-localized state of a conduction electron in an antiferromagnetic semiconductor”, *Sov. Phys. - JETP* **27**, 836 (1968).
- [40] T. Mizokawa, D.I. Khomskii, and G.A. Sawatzky, “Spin and charge ordering in self-doped Mott insulators”, *Phys. Rev. B* **61**, 11263 (2000).
- [41] S. Lee, R. Chen, and L. Balents, “Landau Theory of Charge and Spin Ordering in the Nickelates”, *Phys. Rev. Lett.* **106**, 016405 (2011).
- [42] S.P. Parkin, M. Hayashi, and L. Thomas, “Magnetic domain-wall racetrack memory”, *Science* **320**, 190 (2008).